Наносистеми, наноматеріали, нанотехнології
Nanosistemi, Nanomateriali, Nanotehnologii
2025, т. 23, № 3, сс. 633–651
https://doi.org/10.15407/nnn.23.03.0633

PACS numbers: 28.41.Qb, 61.82.Rx, 78.40.Ha, 78.67.Sc, 81.05.Je, 87.50.-a, 87.85.jf

Applications of EMI Shielding: A Review on the Role of MXenes and Their Composites

N. V. Krishna Prasad

Department of Physics (GSS),
GITAM Deemed to be University,
562163 Bangalore, India

MXenes are emerging materials that find significant applications in EMI shielding. Ferrites, carbon, cotton fabrics, and polymer composites of MXenes are said to improve EMI shielding. These composites are flexible with low weight exhibiting high conductivity and large surface area. The shielding effectiveness depends on parameters like reflection and absorption. Hence, the shielding efficiency may be enhanced by tailoring the MXenes' composite to suitable absorption and multiple reflections. MXenes are two-dimensional materials, which are rapidly expanding in view of their high conductivity, thermal stability, water dispersibility, and easy-process ability. Their effective EMI shielding makes them more significant in electromagnetic applications. This review aims to discuss the shielding effectiveness (SE) obtained by MXenes and their composites. The shielding parameters related to total attenuation (SE_T), attenuation due to absorption (SE_A), attenuation due to reflection (SE_R), and attenuation due to multiple reflections (SE_M) of an electromagnetic wave are discussed. These values determine shielding effectiveness of a given material. If the value of $SE_T \geq 30$ dB, it signifies best efficiency; if $SE_T < 10$ dB, no shielding exists, while, if SE_T is between 10 dB and 30 dB, it denotes minimum effective range of shielding.

Максіни є новітніми матеріялами, які знаходять значне застосування у захисті від електромагнетних завад (ЕМЗ). Вважається, що ферити, вуглець, бавовняні тканини та полімерні композити на основі максінів поліпшують захист від ЕМЗ. Ці композити є гнучкими, легкими та мають високу електропровідність і велику площу поверхні. Ефективність захисту залежить від таких параметрів, як відбивання та вбирання. Тому ефективність захисту може бути підвищена шляхом оптимізації композиту максінів для відповідного вбирання та багаторазового відбивання. Максіни є двовимірними матеріялами, які швидко набирають популярности завдяки високій провідності, термічній стабільності, здатності диспергуватися у воді та легкості оброблянняя. Їхній ефективний захист від ЕМЗ робить їх більш значущими у електромагнетних застосуваннях. Цей огляд має на меті обговорити ефективність екранування (SE), одержану за допомогою максінів та їхніх композитів. Розглядаються параметри екранування, пов'язані із сукупним загасанням (SE_T), загасанням через вбирання (SE_A), загасанням через відбивання (SE_R) та загасанням через багаторазове відбивання (SE_M) електромагнетної хвилі. Ці значення визначають ефективність екранування конкретного матеріялу. Якщо значення $SE_T \geq 30$ дБ, це означає найвищу ефективність; якщо $SE_T < 10$ дБ, екранування відсутнє, а якщо SE_T знаходиться між 10 дБ і 30 дБ, це означає мінімально ефективний рівень екранування.

Key words: MXenes, MXenes' composites, EMI shielding, shielding effectiveness.

Ключові слова: максіни, композити максінів, екранування від електромагнетних завад, ефективність екранування.

(Received 5 March, 2024)

1. INTRODUCTION

High-frequency electromagnetic waves in the range of gigahertz harm commercial IT devices and defence devices due to interference with devices input signal [1]. This type of interference is called electromagnetic interference (EMI), which leads to EMI pollution. This phenomenon affects the efficiency and durability of the device. Besides this, human health will be affected by EMI pollution that includes cancer. It is inevitable to save humankind and electronic devices from this EMI pollution. Hence, shielding of electromagnetic interference using certain materials is of prime importance. Shielding materials may be classified into metals, which exhibit reflection, as well as absorption ferrites, which have absorption only [2, 3]. Shielding by reflection utilizes Faraday's cage principle and by absorption dealing with permeability [4, 5]. The main principle behind EMI shielding is to design an effective material (shield) that reflects incoming electromagnetic waves or to absorb energy in the form of heat. Figure 1 shows the mechanism of EMI shielding [6]. As shown in this figure, the incident electromagnetic waves are reflected by the shields' surface.

The extent of reflection depends on the electron density (availability of free electrons) and conductivity. It is reported that the EM waves will be reflected, if the shielding material is highly conductive with large number of charge carriers [7]. If a shield with reflection dominance is used, the effectiveness will be reduced due to creation of secondary waves. To overcome this drawback, shields

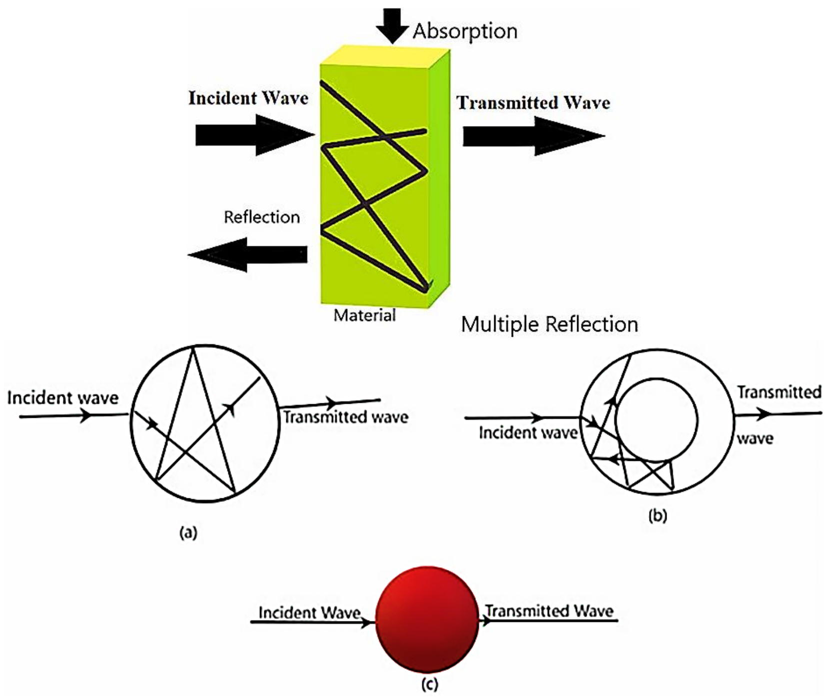

Fig. 1. EMI-shielding mechanism (*a*, *b*) [6].

with absorption dominance with varying dielectric and magnetic losses are preferred [8–10]. Graphene and MXenes prove to be potential materials for EMI shielding [11, 12]. It is reported that foaming materials (foamed polymers blended with carbon nanotubes (CNTs)) effectively enhance dispersion, which improves shielding efficiency [3]. Highly conductive MXenes lead the race due to limited usage of graphene/carbon-based materials [13, 14].

High metallic conductivity, mechanical flexibility, and customizable surface chemistry of MXenes made them rapidly growing [15–17]. The path travelled by electromagnetic waves in the shield and the energy dissipated prior to transmission depend on the structural design [18–20]. Apart from this, heat dissipation may affect stability and duration of the device [21]. This drawback can be minimised by using MXenes having layered structure and high temperature stability [22]. In addition, secondary reflections affect environment that can be overcome through green EMI shielding. In this context, development of green M-$Ti_3C_2T_x$ MXene/hydroxyethyl cellulose composite film was of importance. This film exhibited good shielding performance confirming absorption-dominant EMI shielding [23]. Hence, absorption dominated MXenes' composites are preferred for EMI shielding over secondary reflections. Based on the above brief introduction, we provided a comprehensive analysis regarding the role of MXenes and their composites in EMI shielding with focus on high-frequency devices.

2. PARAMETERS OF EMI SHIELDING

EMI-shielding effectiveness (SE) is given by the ratio of transmitted power P_t and incident power P_i: $SE = 10\log P_t/P_i$. It is reported that the total EMI-shielding effectiveness (SET) is purely a function of SE_A (absorption loss), SE_R (reflection loss) and SE_M (multiple reflection loss) of electromagnetic waves, which propagate through the shielding material (Schelkunoffs theory). The total shielding effectiveness is given by $SE_T = SE_A + SE_R + SE_M$.

3. STRUCTURE OF MXenes

MXenes (pronounced as 'max-eens') are 2*D* nanomaterials discovered in 2011. They belong to ceramics class within the 2*D* materials. MXenes are made of bulk crystal MAX. Their structure consists of molecular sheets derived from titanium nitrides and titanium carbides making them exhibit high conductivity and volumetric capacitance inherently. MXenes are known for various applications in medicine, sensing, and energy storage, *etc*. MXenes can be easily structured by ordering millions of carbon, transition metals, and nitrogen with emphasis on stable arrangement. These ceramics produce 3*D* materials, when substituted with Ti_3AlC_2 powder in hydrofluoric acid through selective removal of aluminium. Two-dimensional Ti_3C_2 nanosheets (MXenes) can be derived through exfoliation. MXene is similar to graphene with different properties. MXene was first demonstrated in 2011 by transforming the three-dimensional Ti_3AlC_2 materials representing MAX phase into a 2*D* material [24]. Figure 2 displays the journey of MXenes during 2011–2021.

MXenes gained prominence with high conductivity and mechanical flexibility as compared to other materials. They can be moulded into nanoparticles, nanosheets of single layer and multilayers. MXenes easily form composites with other materials. The structure of MXenes enhances their mechanical flexibility and stretch ability making them feasible for EMI shielding.

MXenes are derived from MAX phases, whose formula is given by $M_{n+1}AX_n$, where 'n' = 1, ..., 4; 'M' represents early transition metal, 'A' represents A-group element, 'X' represents nitrogen or carbon.

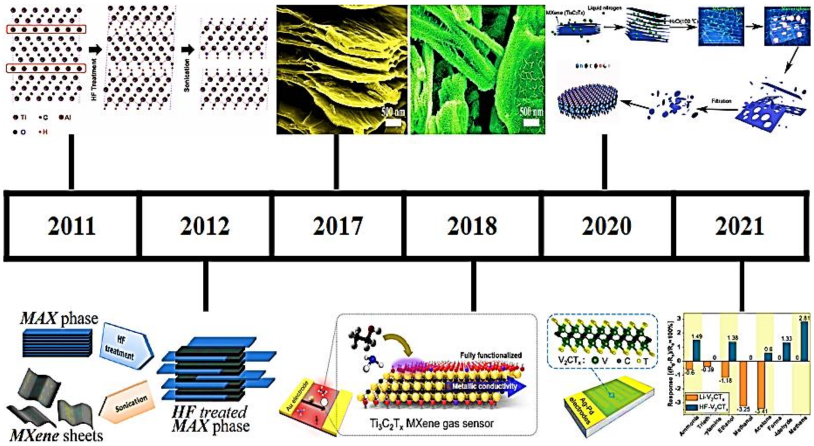

Fig. 2. Journey of MXenes from 2011 to 2021 [25].

They have edge-sharing structure with distorted XM_6 octahedral loaded by single planar layers of A-group element [26]. 3D MAX-phase structure is displayed in Fig. 3.

MXenes are derived from MAX phases through selective etching of A layers (Fig. 4). Different preparation methods for MXenes are reported in Ref. [28].

4. MXenes in EMI Shielding

High electrical conductivity is required for any material to be used as EMI shield. 2D MXenes can be processed to have large surface area and low density as compared to heavy metals, stretch ability (foldable devices), and easy-process ability [29]. Conductivity of two-dimensional MXenes ranges between 5 to 20 000 S/cm based on composition with least conductivity required being 1 S/cm [30]. MXene films possess high electrical conductivity with multilayered 2D MXene sheets. This structure helps them to absorb the incident electromagnetic wave as compared to conventional shielding materials. Various forms of MXene films are available and are capable of attenuating the energy with efficient shielding. MXene with a single layer having 2.3 nm thickness could prevent EM interference [31]. With suitable modification of MXenes' structure by adding pores or dielectric domains, reflections from multiple interfaces in the shield can be enhanced that reduces the strength of electromagnetic waves. In addition, electromagnetic-waves' absorption can be achieved by increasing polarization losses through chemical composition. Using the technique of capacitive loss, dipoles can be produced by negatively charged surface on applying electromagnetic

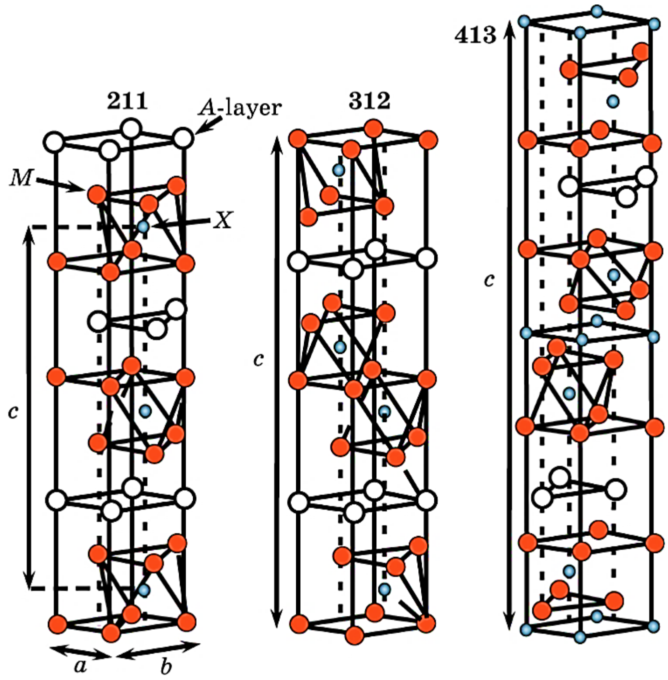

Fig. 3. Crystal structure of MAX phases [27].

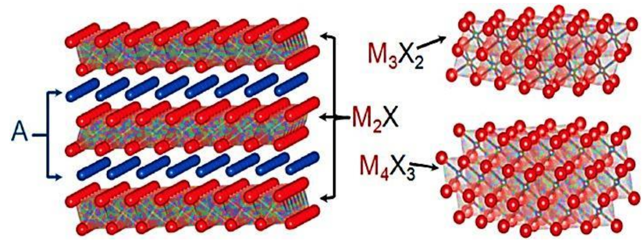

Fig. 4. Representation of MAX phase [6].

field to reduce its energy [32, 33]. This is due predominance of dipolar polarization gigahertz-frequency range. These characteristics signify MXenes as potential materials for EMI shielding in electronic devices.

The impact of heat treatment after etching on dielectric and wave absorption on MXene was reported. Fifty percent annealed MXenes exhibit a minimum reflection loss of −48.4 dB at 11.6 GHz with good absorbance and shielding. MXenes of unit thickness exhibited 76.1 dB, when untreated, and 67.3 dB, when annealed. Absorbing and total shielding effectiveness values were found to be 24.2 dB

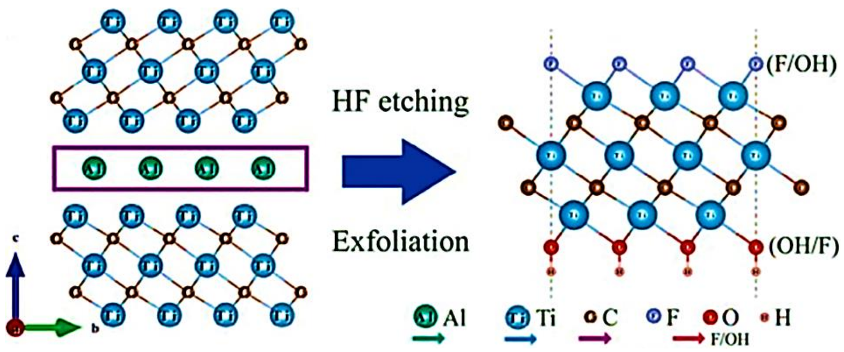

Fig. 5. MXenes with various functional groups [6].

and 32 dB [34]. MXene of 0.8 mm-thickness with sandwich structure demonstrated EMI-shielding effectiveness above 70 dB in *X*-band [35]. MXene with large area, smooth surface, and high electrical conductivity exhibited the mean and absolute shielding effectivenesses equal to 55.7 dB and 48.800 $dB \cdot cm^2 \cdot g^{-1}$. These results indicate that EMI-shielding effectiveness of MXenes may be enhanced with different manufacturing techniques [36]. Hence, it can be inferred that MXenes can be considered EMI shields. As *per* the mentioned examples, large surface area, multilayered structure, and high electrical conductivity of MXenes significantly contribute to increase EMI shielding.

4.2. MXenes and Polymer Composites in EMI Shielding

Conductive polymer composites (CPCs) with conductive fillers are highly considered for EMI shielding. They are of lightweight, economical, resistive to corrosion and can be easily processed [37–40]. Even though these materials exhibit high electrical conductivity, increased impedance mismatch and dielectric loss act as major drawback [41, 42]. In addition, CPCs filled with fillers are thick and not adaptable to use and lose their mechanical strength. Hence, MXene and polymer composites, wherein the polymer acting as binder increases the mechanical strength, make them suitable for EMI-shielding materials [43]. This combination was first tested in 2018. An ultrathin MXene/cellulose nanofibres-composite paper with excellent mechanical property reported tensile strength of 135.4 MPa and strain near to 16.7% [44]. These materials can be used in robot joints, weapon equipment, and flexible electronics. Similarly, a composite of polyvinylidenefluoride, MXene and nickel was synthesized and reported with good EMI-shielding properties [45]. In addition, multilayered films of MXene, polydimethylsilox-

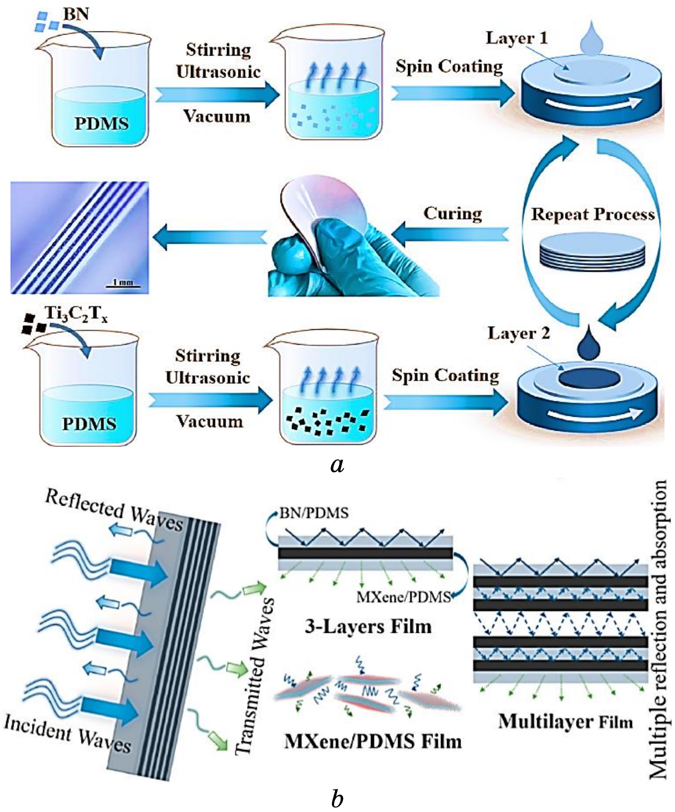

Fig. 6. Synthesis (*a*) and shielding (*b*) mechanism of MXene, PDMS and BN composites [6, 44].

ane (PDMS) and boron nitride were synthesized with spin-coating method.

Figure 6, *a* [46] shows the synthesis and Fig. 6, *b* shows the shielding mechanism of the prepared film. These films reported SE of 35.2 dB for an 11-layered material with thermal conductivity of 3.29 kV/mm at 10.9 GHz. In addition, SE_A was greater than SE_R.

Figure 6, *b* explains the mechanism behind this effect. As shown in this figure, electromagnetic waves, which are incident on BN/PDMS layer, are penetrated directly. The waves, which strike PDMS/MXene, are divided into two beams, in which one beam reflects back and the remaining part transmits through the interior layer. The existence of alternative multilayer enhances the quantity of reflection and scattering, which attenuates the waves continuously. Hence, it is inferred that SE depends on the number of MXene/PDMS layers. Considering this, fabrication of less-layered $Ti_3C_2T_x$/epoxy composites using casting method, was reported [47].

In addition, SE was of 41 dB with 15% loading, when annealed. This was by 37% higher as compared to without annealing. This can be attributed to formation of large number of dipoles post annealing.

4.3. MXenes and Cotton Fibre Composites in EMI Shielding

Cotton and their composites are becoming prominent in view of their advantages over synthetic textiles [48–50]. Electronic equipment with conductive cotton fabrics has the ability of blocking electromagnetic radiation [51, 52]. However, the main drawback of cotton is its flammability, when used in electronic equipment. Hence, it is preferable to use materials, which are flame resistant for EMI shielding. In this context, EMI-shielding cotton textiles developed with aqueous impregnation and dip coating are of importance [53]. Three-layered combination of MXene, ammonium phosphate and polyacetimidate could increase conductivity from unity to 670 S/m by increasing MXenes. This addition of MXene sheets to cotton fibre makes the fibre to act as a conducting body. In extension to this, a conductive network of cotton fabrics was reported [54].

As shown in Fig. 7, MXenes are modified by adhering fabric surfaces. These fabrics exhibit high conductivity, Joule heating capability at 150°C with 6 V supply and are reported to block EM interference. In addition, they can be used as strain sensors to track the activity of humans. In this sequence, waste fibres of cotton were

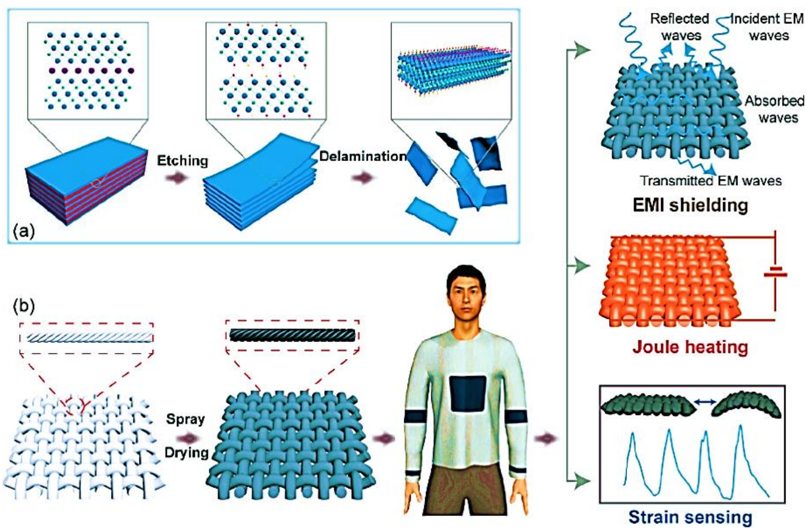

Fig. 7. Preparation of modified cotton fabrics and its applications [6, 52].

converted to aerogels by dissolving them in aqueous solution of NaOH/urea. These aerogels were combined with MXene nanosheets through dip coating to develop the woven carbon fibres/MXene composites [55].

These composites exhibit an effectiveness of 39-to-48 dB between 2 GHz and 18 GHz. As mentioned earlier to avoid flammable issues, a combination of MXene with inflammable aramid non-woven fabric was developed [56]. In this order, composites of MXene, polyaniline (PANI) and cotton fabric were developed that increased shielding effectiveness by 54 dB [57]. Similar developments include lightweight non-woven fabrics combined with MXenes, which were absorption dominant [58]. Based on the number of fabric layers, conductivity increased from 5.04 S/m to 13.45 S/m with optimum effectiveness of 25.26 dB at 12.4 GHz [59].

Even though cotton fabrics show increase in ohmic loss because of being porous and absorb incoming radiation; their poor heat resistance and low mechanical-strength challenge their EMI-shielding characteristics.

4.4. MXenes and Carbon-Derivatives' Composites in EMI Shielding

Carbon and its derivatives play an important role in EMI shielding [60–62]. $3D$ structure and other characteristics made these materials significant. However, porous nature and weak hydrogen bonding make these materials to have low mechanical strength [63]. To avoid this drawback, porous carbon composites using very thin aerogel of MXene and wood were designed [64]. This enhanced the required mechanical strength and SE_T was found to be of 69.4 dB. This could achieve a shielding effectiveness of 71.3 dB. In continuation, spin layered-composite films with MXene and CNTs were reported [65]. Similarly, a lightweight-layered fabric with MXene and PANI polymer was prepared and checked for shielding effectiveness and Joule heating. SE_A and SE_R are reported to increase with assembly cycles [66]. MXene and CNTs composite of 100-μm thickness prepared with facile electron deposition demonstrated an effectiveness of 60.5 dB in X-band [67]. SE decreases to 50.4 dB, if the thickness was reduced to 15 μm. The mechanism behind this high shielding is due to reflection of EM waves on reaching the high-conductive hybrid surface, as shown in Fig. 8.

$2D$ composites of MXene and graphene nanoplatelets of 1.75-m thickness exhibited 64 dB electromagnetic absorbance between 60–80 GHz) [68]. MXenes being highly potential for EMI shielding and, as graphene, exhibit good electrical conductivity, low density, and corrosion resistant; their combination leads to excellent applications in EMI shielding.

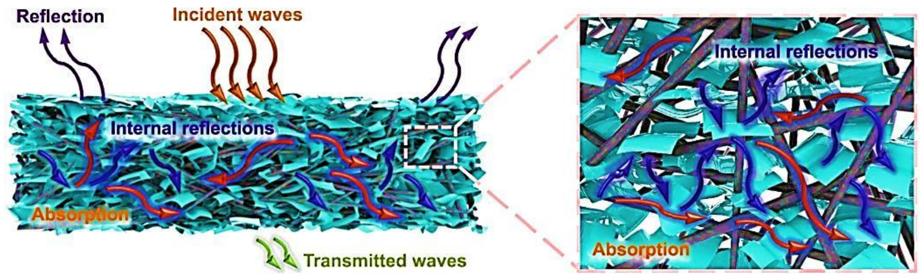

Fig. 8. EMI-shielding mechanism for MXene and CNTs composites [6, 65, 95].

4.5. MXenes and Ferrite Composites in EMI Shielding

Low magnetic losses in MXenes make them poor electromagnetic-wave absorbers. Hence, magnetic losses need to be enhanced [69–72]. This can be achieved with the help of magnetic nanoparticles [73]. Observations indicated that spinel ferrites possess superior magnetic properties and, if coupled with MXenes, yield good results [74–78]. MXene and $Ni_{0.5}Zn_{0.5}Fe_2O_4$ composites prepared with co-precipitation method yielded saturation magnetization of 27.08 emu/g. MXene and Ni–Zn ferrite composites were reported to be effective shields [79]. Different composites of this combination with excellent absorption that could be used in 5G networks were reported [80–88]. MXene and $Ni_{0.6}Zn_{0.4}Fe_2O_4$ (NZFO) nanocomposites with reflection loss (RL_{min}) of 66.2 dB at frequency of 15.2 GHz and 4.74 GHz bandwidth were reported. These composites simulate the properties of double-loss electromagnetic absorbing material with strong reflection loss [89]. This loss was attributed to impedance matching. The mechanism behind this was shown in Fig. 9. As

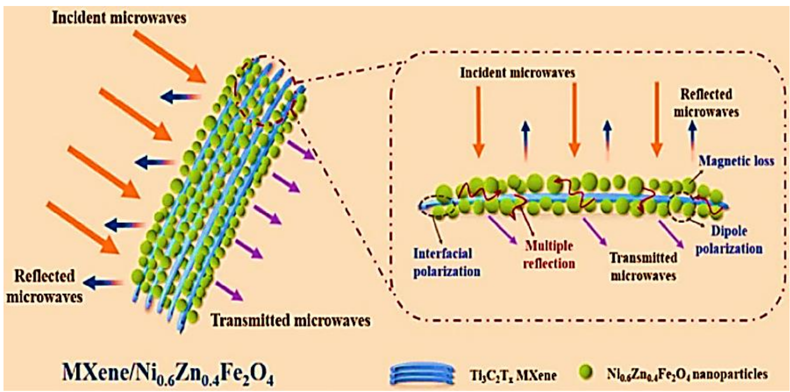

Fig. 9. EMI-shielding mechanism for MXene/NZFO composites [6].

shown in this figure, impedance matching favours reflection of incident waves. Various interfaces between MXene layers improve interfacial polarization contributing to dielectric relaxation. Numbers of dipoles are generated due to large number of MXene-surface termination groups leading to dipolar polarization and, finally, interaction between magnetic and dielectric losses that enhances electromagnetic-wave absorption. Hence, combination of MXenes with ferrite nanoparticles improves EMI shielding.

4.6. MXenes and MOF Composites in EMI Shielding

In view of the limitations exhibited by MXene over its own composites, a composite of MXene with metal–organic frameworks (MOFs) was considered. MOFs have metal-ion terminals connected with organic ligands. They benefit from high porosity and large specific surface area, which make them suitable for energy storage [90–92]. $Co/ZnO/Ti_3C_2T_x$ MXene/MOFs composites were prepared. They reported improvement in morphology due to interaction of MOFs with MXene possessing excellent dielectric and magnetic losses [93]. Similarly, an intertwined one-dimensional heterostructure with MXene and cobalt–nickel MOFs was reported. Three-dimensional structures with CNTs with a matching thickness of 1.6 mm could exceed RL_{min} by 51.6 dB and 4.6 GHz for embedded array blocks (EAB) [94]. The mechanism behind these absorption properties was shown in Fig. 10. As shown in this figure, interaction between MXene, MOFs and CNTs lead to good attenuation and impedance matching promoting interface polarization improving microwave absorption. Porous structure of this combination enhances scattering and multiple reflections of incident EM waves.

5. CONCLUSIONS

EMI shielding has gained significance in protecting human beings and electronic devices from pollution due to electromagnetic radiation. Even though various materials are used for EMI shielding, MXenes gained prominence in recent times. High conductivity, good thermal stability, surface chemistry, and simple-process ability of these materials make them crucial in EMI-shielding applications. Since MXenes alone could not satisfy the criteria required by EMI shielding, combination of MXenes with other shielding materials was in the radar of researchers. Keeping this in mind, an attempt was made to review the reported publications, which analysed the role of MXenes and their composites in EMI shielding in a nutshell. It was observed that, among the cotton fabrics, fabrics made of

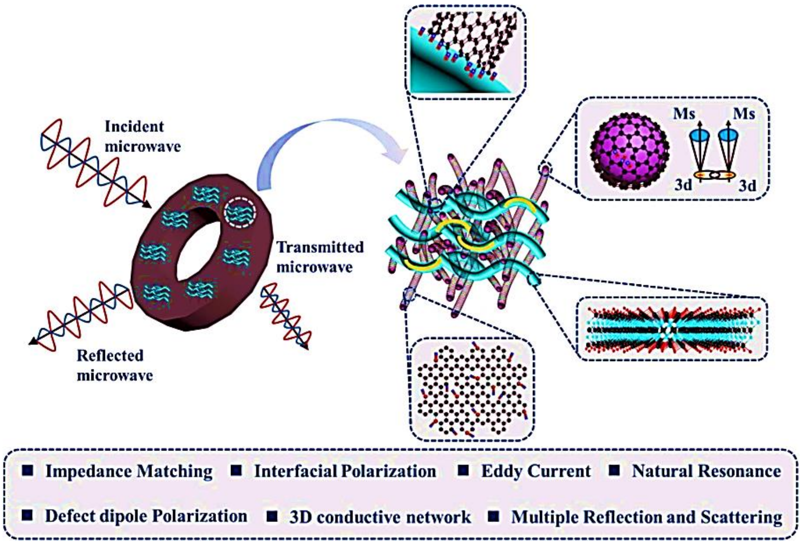

Fig. 10. Schematic mechanism of EMI-shielding performance of Co–Ni-bimetal MOFs/MXene [6, 94].

MXenes and wood pulp show highest SE of 90.2 dB. Improved shielding was seen in case of MXenes combined with cotton fabrics, polymers, and ferrite nanoparticles. Hence, they may be used in IT and defence sectors. In addition, various composites in combination with MXenes suitable for EMI shielding were discussed.

ACKNOWLEDGEMENTS

The author sincerely acknowledges Ritesh Verma *et al.* (2023) for giving the copyright to use the images in this review article.

REFERENCES

1. S. Geetha, K. K. S. Kumar, C. R. K. Rao, M. Vijayan, and D. C. Trivedi, *J. Appl. Polym. Sci.*, **112**, Iss. 4: 2073 (2009); doi:10.1002/app.29812
2. Meikang Han and Yury Gogotsi, *Carbon*, **204**: 17 (2023); doi:10.1016/j.carbon.2022.12.036
3. Yue-Yi Wang, Feng Zhang, Nan Li, Jun-Feng Shi, Li-Chuan Jia, Ding-Xiang Yan, and Zhong-Ming Li, *Carbon*, **205**: 10 (2023); doi:10.1016/j.carbon.2023.01.007
4. Khalid Muajsam Batoo, Muhammad Hadi, Ritesh Verma, Ankush Chauhan, Rajesh Kumar, Mahavir Singh, and Omar M. Aldossary, *Ceram. Int.*, **48**, Iss. 3: 3328 (2022); doi:10.1016/j.ceramint.2021.10.108
5. Khalid Mujasam Batoo, Muhammad Hadi, Ankush Chauhan, Ritesh Verma,

Mahavir Singh, Omar M. Aldossary, and Gagan Kumar Bhargava, *Appl. Phys. A*, **128**: Article No. 283 (2022); doi:10.1007/s00339-022-05423-1
6. Ritesh Verma, Preethi Thakur, Ankush Chauhan, Rohit Jasrotia, and Atul Thakur, *Carbon*, **208**: 170 (2023); doi:10.1016/j.carbon.2023.03.050
7. Y. S. Choi, Y. H. Yoo, J. G. Kim, and S. H. Kim, *Surf. Coating. Technol.*, **201**: 6 (2006); doi: 10.1016/j.surfcoat.2006.03.040
8. Aamir Iqbal, Faisal Shahzad, Kanit Hantanasirisakul, Myung-Ki Kim, Jisung Kwon, Junpyo Hong, Hyerim Kim, Daesin Kim, Yury Gogotsi, and Chong Min Koo, *Science*, **369**, Iss. 6502: 446 (2020); doi:10.1126/science.aba7977
9. Seung Hwan Lee, Seunggun Yu, Faisal Shahzad, Woo Nyon Kim, Cheolmin Park, Soon Man Hong, and Chong Min Koo, *Nanoscale*, **36**: 13432 (2017); doi:10.1039/C7NR02618H
10. Hongtao Guan and D. D. L. Chung, *Carbon*, **157**: 549 (2020); doi:10.1016/j.carbon.201910.071
11. Aamir Iqbal, Pradeep Sambyal, and Chong Min Koo, *Adv. Funct. Mater.*, **30**: Iss. 47: 2000883 (2020); doi:10.1002/adfm.202000883
12. Ji Liu, Hao-Bin Zhang, Renhui Sun, Yafeng Liu, Zhangshuo Liu, Aiguo Zhou, and Zhong-Zhen Yu, *Adv. Mater.*, **29**: Iss. 38: 1702367 (2017); doi:10.1002/adma.201702367
13. Pradip Kumar, Seunggun Yu, Faisal Shahzad, Soon Man Hong, Yoon-Hyun Kim, and Chong Min Koo, *Carbon*, **101**: **120** (2016); doi:10.1016/j.carbon.2016.01.88
14. Pradip Kumar, Faisal Shahzad, Seunggun Yu, Soon Man Hong, Yoon-Hyun Kim, and Chong Min Koo, *Carbon*, **94**: 494 (2015); doi:10.1016/j.carbon.2015.07.032
15. Jizhen Zhang, Na Kong, Simge Uzun, Ariana Levitt, Shayan Seyedin, Peter A. Lynch, Si Qin, Meikang Han, Wenrong Yang, Jingquan Liu, Xungai Wang, Yury Gogotsi, and Joselito M. Razal, *Adv. Mater.*, **32**, Iss. 23: 2001093 (2020); doi:10.1002/adma.202001093
16. Min Su Kim, Seongyeon Cho, Se Hun Joo, Junsang Lee, Sang Kyu Kwak, Moon Il Kim, and Jinwoo Lee, *ACS Nano*, **13**, Iss. 4: **4312** (2019); doi:10.1021/acsnano.9b04088
17. Pradeep Sambyal, Aamir Iqbal, Junpyo Hong, Hyerim Kim, Myung-Ki Kim, Soon Man Hong, Meikang Han, Yury Gogotsi, and Chong Min Koo, *ACS Appl. Mater. Interfaces*, **11**, Iss. 41: 38046 (2019); doi:10.1021/acsami.9b12550
18. Wen-Tao Cao, Fei-Fei Chen, Ying-Jie Zhu, Yong-Gang Zhang, Ying-Ying Jiang, Ming-Guo Ma, and Feng Chen, *ACS Nano*, **12**, Iss. 5: 4583 (2018); doi:10.1021/acsnano.8b00997
19. Guo-Ming Weng, Jinyang Li, Mohamed Alhabeb, Christopher Karpovich, Hang Wang, Jason Lipton, Kathleen Maleski, Jaemin Kong, Evyatar Shaulsky, Menachem Elimelech, Yury Gogotsi, and André D. Taylor, *Adv. Funct. Mater.*, **28**, Iss. 44: 1803360 (2018); doi:10.1002/adfm.201803360
20. Mao-Sheng Cao, Jin-Cheng Shu, Bo Wen, Xi-Xi Wang, and Wen-Qiang Cao, *Small Structures*, **2**, Iss. 11: 2100104 (2021); doi:10.1002/sstr.202100104
21. Maosheng Cao, Xixi Wang, Wenqiang Cao, Xiaoyong Fang, Bo Wen, and Jie Yuan, *Small*, **14**, Iss. 29: 1800987 (2018); doi:10.1002/smll.201800987
22. Xi-Xi Wang, Jin-Cheng Shu, Wen-Qiang Cao, Min Zhang, Jie Yuan, and Mao-Sheng Cao, *Chem. Eng. J.*, **369**: 1068 (2019);

doi:10.1016/j.cej.2019.03.164
23. Peng He, Mao-Sheng Cao, Yong-Zhu Cai, Jin-Cheng Shu, Wen-Qiang Cao, and Jie Yuan, *Carbon*, **157**: 80 (2020); doi:10.1016/j.carbon.2019.10.009
24. Michael Naguib, Murat Kurtoglu, Volker Presser, Jun Lu, Junjie Niu, Min Heon, Lars Hultman, Yury Gogotsi, and Michel W. Barsoum, *Advanced Materials*, **23**, Iss. 37: 4248 (2011); doi:10.1002/adma.201102306
25. Qixun Xia, Yulong Fan, Shiwen Li, Aiguo Zhou, Nanasaheb Shinde, and Rajaram S. Mane, *Diamond and Related Materials*, **131**: 109557 (2023); doi:10.1016/j.diamond.2022.109557
26. Grayson Deysher, Christopher Eugene Shuck, Kanit Hantanasirisakul, Nathan C. Frey, Alexandre C. Foucher, Kathleen Maleski, Asia Sarycheva, Vivek B. Shenoy, Eric A. Stach, Babak Anasori, and Yury Gogotsi, *ACS Nano*, **14**, Iss. 1: 204 (2019); doi:10.1021/acsnano.9b07708
27. Martin Magnuson and Maurizio Mattesini, *Thin Solid Films*, **621**: 108 (2017); doi:10.1016/j.tsf.2016.11.005
28. Rahele Meshkian, Lars-Eke Näslund, Joseph Halim, Jun Lu, Michel W. Barsoum, and Johanna Rosen, *J. Scr. Mater.*, **108**: 147 (2015); doi:10.1016/j.scriptamat.2015.07.003
29. Faisal Shahzad, Mohamed Alhabeb, Christine B. Hatter, Babak Anasori, Soon Man Hong, Chong Min Koo, and Yury Gogotsi, *Science*, **353**, Iss. 6304: 1137 (2016); doi:10.1126/science.aag2421
30. Meikang Han, Christopher Eugene Shuck, Roman Rakhmanov, David Parchment, Babak Anasori, Chong Min Koo, Gary Friedman, and Yury Gogotsi, *ACS Nano*, **14**, Iss. 4: 5008 (2020); doi:10.1021/acsnano.0c01312
31. Hailong Xu, Xiaowei Yin, Xinliang Li, Minghang Li, Shuang Liang, Litong Zhang, and Laifei Cheng, *ACS Appl. Mater. Interfaces*, **11**, Iss. 10: 10198 (2019); doi:10.1021/acsami8b21671
32. Yuan Tong, Man He, Yuming Zhou, Xi Zhong, Lidan Fan, Tingyuan Huang, Qiang Liao, and Yongjuan Wang, *Appl. Surf. Sci.*, **434**: 283 (2018); doi:10.1016/j.apsusc.2017.10.140
33. Meikang Han, Xiaowei Yin, Heng Wu, Zexin Hou, Changqing Song, Xinliang Li, Litong Zhang, and Laifei Cheng, *ACS Appl. Mater. Interfaces*, **8**, Iss. 32: 21011 (2016); doi:10.1021/acsami.6b06*455*
34. Min Li, Yanhui Song, Chao Zhang, Zhenzhong Yong, Jian Qiao, Dongmei Hu, Zuoguang Zhang, Huazhen Wei, Jiangtao Di, and Qingwen Li, *Carbon*, **146**: 627 (2019); doi:10.1016/j.carbon.2019.02.003
35. Jason Lipton, Jason A. Röhr, Vi Dang, Adam Goad, Kathleen Maleski, Francesco Lavini, Meikang Han, Esther H. R. Tsai, Guo-Ming Weng, Jaemin Kong, Elisa Riedo, Yury Gogotsi, and André D. Taylor, *Matter*, **3**: Iss. 2: 546 (2020); doi:10.1016/j.matt.2020.05.023
36. Zhihui Zeng, Hao Jin, Mingji Chen, Weiwei Li, Licheng Zhou, and Zhong Zhang, *Adv. Funct. Mater.*, **26**, Iss. 2: (2016); doi:10.1002/adfm.201503579
37. Di Xing, Longsheng Lu, Kwok Siong Teh, Zhenping Wan, Yingxi Xie, and Yong Tang, *Carbon*, **132**: 32 (2018); doi:10.1016/j.carbon.2018.02.001
38. Yuezhan Feng, Bo Wang, Xiongwei Li, Yunsheng Ye, Jianmin Ma, Chuntai Liu, Xingping Zhou, and Xiaolin Xie, *Carbon*, **146**: 650 (2019); doi:10.1016/j.carbon.2019.01.099
39. Yuezhan Feng, Gaojie Han, Bo Wang, Xingping Zhou, Jianmin Ma, Yunsheng Ye, Chuntai Liu, and Xiaolin Xie, *Chem. Eng. J.*, **379**: 122402

(2019); doi:10.1016/j.cej.2019.122402
40. Xian-feng Meng, Dong-hong Li, and Xiang-qian Shen, and Wei Liu, *Appl. Surf. Sci.*, **256**, Iss. 12: 3753 (2010); doi:10.1016/j.apsusc.2010.01.019
41. Min Li, Yanhui Song, Chao Zhang, Zhenzhong Yong, Jian Qiao, Dongmei Hu, Zuoguang Zhang, Huazhen Wei, Jiangtao Di, and Qingwen Li, *Carbon*, **146**: 627 (2019); doi:10.1016/j.carbon.2019.02.003
42. Wen-Tao Cao, Fei-Fei Chen, Ying-Jie Zhu, Yong-Gang Zhang, Ying-Ying Jiang, Ming-Guo Ma, and Feng Chen, *ACS Nano*, **12**: Iss. 5: 4583 (2018); doi:10.1021/acsnano.8b00997
43. Shi-Jun Wang, Dian-Sen Li, and Lei Jiang, *Adv. Mater. Interfac.*, **6**, Iss. 19: 1900961 (2019); doi:10.1002/admi.201900961
44. Houbao Liu, Renli Fu, Xinqing Su, Binyong Wu, He Wang, Yue Xu, and Xuhai Liu, *Compos. Commun.*, **23**: 100593 (2021); doi:10.1016/j.coco.2020.100593
45. Lei Wang, Lixin Chen, Ping Song, Chaobo Liang, Yuanjin Lu, Hua Qiu, Yali Zhang, Jie Kong, and Junwei Gu, *Composites Part B*: *Engineering*, **171**: 111 (2019); doi:10.1016/j.compositesb.2019.04.050
46. Ruiting Liu, Miao Miao, Yahui Li, Jianfeng Zhang, Shaomei Cao, and Xin Feng, *ACS Appl. Mater. Interfaces*, **10**, Iss. 51: 44787 (2018); doi:10.1021/acsami.8b18347
47. Zhaoqing Lu, Fengfeng Jia, Longhai Zhuo, Doudou Ning, Kun Gao, and Fan Xie, *Composites Part B: Engineering*, **217**: 108853 (2021); https://doi.org/10.1016/j.compositesb.2021.108853
48. Jia-Qi Luo, Sai Zhao, Hao-Bin Zhang, Zhiming Deng, Lulu Li, and Zhong-Zhen Yu, *Comput. Sci. Technol.*, **182**: 107754 (2019); doi:10.1016/j.compscitech.2019.107754
49. Ying Shang, Youxin Ji, Jingwen Dong, Gui Yang, Xiaodong Zhang, Fengmei Su, Yuezhan Feng, and Chuntai Liu, *Compos. Sci. Technol.*, **214**: 108974 (2021); doi:10.1016/j.compscitech.2021.108974
50. Hailong Xu, Xiaowei Yin, Xinliang Li, Minghang Li, Shuang Liang, Litong Zhang, and Laifei Cheng, *Appl. Mater. Interf.*, **11**, Iss. 10: 10198 (2019); doi:10.1021/acsami.8b21671
51. Wenhua Cheng, Yan Zhang, Wenxiang Tian, Jiajia Liu, Jingyi Lu, Bibo Wang, Weiyi Xing, and Yuan Hu, *Ind. Eng. Res.*, **59**, Iss. 31: 14025 (2020); doi:10.1021/acs.iecr.0c02618
52. Xiansheng Zhang, Xifeng Wang, Zhiwei Lei, Lili Wang, Mingwei Tian, Shifeng Zhu, Hong Xiao, Xiaoning Tang, and Lijun Qu, *ACS Appl. Mater.*, **12**, Iss. 12: 14459 (2020); doi:10.1021/acsami.0c01182
53. Jianyu Zhai, Ce Cui, Ang Li, Ronghui Guo, Cheng Cheng, Erhui Ren, Hongyan Xiao, Mi Zhou, and Jinwei Zhang, *Ceram. Int.*, **48**, Iss. 10: 13464 (2022); doi:10.1016/j.ceramint.2022.01.224
54. Xifeng Wang, Zhiwei Lei, Xianda Ma, Guifang He, Tong Xu, Jing Tan, Lili Wang, Xiansheng Zhang, Lijun Qu, and Xueji Zhang, *Chem. Eng. J.*, **430**, Pt. 1: 132605 (2022); doi:10.1016/j.cej.2021132605
55. Dan-Yang Li, Liu-Xin Liu, Qi-Wei Wang, Hao-Bin Zhang, Wei Chen, Guang Yin, and Zhong-Zhen Yu, **14**, Iss. 10: 12703 (2022); doi:10.1021/acsami.2c00797
56. Xinli Liu, Jisi Wu, Jun He, and Lei Zhang, *Mater. Lett.*, **205**: 261 (2017); doi:10.1016/j.matlet.2017.06.101

57. Hengyu Zhang, Jianying Chen, Hui Ji, Ni Wang, Shuo Feng, and Hong Xiao, *Textil. Res. J.*, **91**, Iss. 21–22: 1 (2021); doi:10.1177/00405175211006216
58. Ye Yuan, Weilong Yin, Minglong Yang, Fan Xu, Xu Zhao, Jianjun Li, Qingyu Peng, Xiaodong He, Shanyi Du, and Yibin Li, *Carbon*, **130**: 59 (2018); doi:10.1016/j.carbon.2017.12.122
59. Polina P. Kuzhir, Alesia G. Paddubskaya, Nadezhda I. Volynets, Konstantin G. Batrakov, Tommi Kaplas, Patrizia Lamberti, Rumiana Kotsilkova, and Philippe Lambin, *J. Nanophotonics*, **11**: Iss. 3: 032504 (2017); doi:10.1117/1.JNP.11.032504
60. Qin-Yi Li, Tianli Feng, Wakana Okita, Yohei Komori, Hiroo Suzuki, Toshiaki Kato, Toshiro Kaneko, Tatsuya Ikuta, Xiulin Ruan, and Koji Takahashi, *ACS Nano*, **13**: Iss. 8: 9182 (2019); doi:10.1021/acsnano.9b03521
61. Xiaohui Ma, Bin Shen, Lihua Zhang, Zeping Chen, Yinfeng Liu, Wentao Zhai, and Wenge Zheng, *ACS Sustain. Chem. Eng.*, **7**, Iss. 10: 9663 (2019); doi:10.1021/acssuschemeng.9b01288
62. Chaobo Liang, Hua Qiu, Ping Song, Xuetao Shi, Jie Kong, and Junwei Gu, *Sci. Bull.*, **65**: Iss. 8: 616 (2020); doi:10.1016/j.scib.2020.02.009
63. Guo-Ming Weng, Jinyang Li, Mohamed Alhabeb, Christopher Karpovich, Hang Wang, Jason Lipton, Kathleen Maleski, Jaemin Kong, Evyatar Shaulsky, Menachem Elimelech, Yury Gogotsi, and André D. Taylor, *Adv. Funct. Mater.*, **28**: Iss. 44: 1803360 (2018); https://doi.org/10.1002/adfm.201803360
64. Guang Yin, Yu Wang, Wei Wang, and Dan Yu, *Colloids Surf. A*, **601**: 125047 (2020); https://doi.org/10.1016/j.colsurfa.2020.125047
65. Rongliang Yang, Xuchun Gui, Li Yao, Qingmei Hu, Leilei Yang, Hao Zhang, Yongtao Yao, Hui Mei, and Zikang Tang, *Nano-Micro Lett.*, **13**: Arrticle No. 66 (2021); doi:10.1007/s40820-021-00597-4
66. B. Aïssa, A. Sinopoli, A. Ali, Y. Zakaria, A. Zekri, M. Helal, M. Nedil, F. Rosei, S. Mansour, and K. A. Mahmoud, *Carbon*, **173**: 528 (2021); doi:10.1016/j.carbon.2020.11.024
67. Peng Yan, Fanrong Ai, Chuanliang Cao, and Zhongmin Luo, *J. Mater. Sci. Mater. Electron.*, **30**: 14120 (2019); doi: 10.1007/s10854-019-00959-0
68. Heng Luo, Wanlin Feng, Congwei Liao, Lianwen Deng, Sheng Liu, Haibin Zhang, and Peng Xiao, *J. Appl. Phys.*, **123**: 104103 (2018); doi:10.1063/1.5008323
69. Caiyun Liang and Zhijiang Wang, *Chem. Eng. J.*, **373**: 598 (2019); doi:10.1016/j.cej.2019.05.076
70. Xinliang Li, Xiaowei Yin, Changqing Song, Meikang Han, Hailong Xu, Wenyan Duan, Laifei Cheng, and Litong Zhang, *Adv. Funct. Mater.*, **28**, Iss. 41: 1803938 (2018); doi:10.1002/adfm.201803938
71. Wanlin Feng, Heng Luo, Sifan Zeng, Chen Chen, Lianwen Deng, Yongqiang Tan, Xiaosong Zhou, Shuming Peng, and Haibin Zhang, *Mater. Chem. Front.*, **2**: 2320 (2018); doi:10.1039/C8QM00436F
72. Sonam Kumari, Neetu Dhanda, Atul Thakur, Satyendra Singh, and Preeti Thakur, *Mater. Chem. Phys.*, **297**: 127394 (2023); doi:10.1016/j.matchemphys.2023.127394
73. Shilpa Taneja, Deepika Chahar, Preeti Thakur, and Atul Thakur, *J. Alloys Compd.*, **859**: 157760 (2021); doi:10.1016/j.jallcom.2020.157760

74. Pinki Punia, Preeti Thakur, Rakesh Kumar, Rajat Syal, Rakesh Dhar, and Atul Thakur, *J. Alloys Compd.*, **928**: 167248 (2022); doi:10.1016/j.jallcom.2022.167248
75. Shilpa Taneja, Preeti Thakur, Blaise Ravelo, and Atul Thakur, *Mater. Res. Bull.*, **154**: 111937 (2022); doi:10.1016/j.materresbull.2022.111937
76. *Synthesis and Applications of Nanoparticles* (Eds. Atul Thakur, Preeti Thakur, and S. M. Paul Khurana) (Singapore: Springer: 2022).
77. Hua-Yao Li, Liang Huang, Xiao-Xue Wang, Chul-Soon Lee, Ji-Wook Yoon, Jun Zhou, Xin Guo, and Jong-Heun Lee, *RSC Adv.*, **7**: 3680 (2017); doi:10.1039/C7RA03402D
78. Baiwen Deng, Lihao Wang, Zhen Xiang, Zhicheng Liu, Fei Pan, and Wei Lu, *Mater. Lett.*, **284**, Pt. 1: 129029 (2021); https://doi.org/10.1016/j.matlet.2020.129029
79. Yiming Lei, Zhengjun Yao, Shuzhou Li, Jintang Zhou, Azhar Ali Haidry, and Peijiang Liu, *Ceram. Int.*, **46**: Iss. 8, Pt. A: 10006 (2020); https://doi.org/10.1016/j.ceramint.2019.12.189
80. Hua Qiu, Xian Luo, Jin Wang, Xiaolan Zhong, and Shuhua Qi, *J. Electron. Mater.*, **48**: 4400 (2019); doi:10.1007/s11664-019-07220-8
81. Erqi Yang, Xiaosi Qi, Hongbo Cai, Ren Xie, Zhongchen Bai, Yang Jiang, Shuijie Qin, Wei Zhong, and Youwei Du, *Mater. Sci. Eng. B*, **238–239**: 7 (2018); doi:10.1016/j.mseb.2018.12.009
82. Zhen Wang, Zhi Cheng, Li Xie, Xianliang Hou, and Changqing Fang, *Ceram. Int.*, **47**, Iss. 4: 5747 (2021); doi:10.1016/j.ceramint.2020.10.161
83. Hoyun Won, Yang-Ki Hong, Minyeong Choi, Hector Garcia, Dongmyung Shin, Young-Sik Yoon, Kwangjoo Lee, Hao Xin, and Chang-Dong Yeo, *J. Magn. Magn. Mater.*, **560**: 169523 (2022); doi:10.1016/j.jmmm.2022.169523
84. Sumit Kumar, Parveen Kumar, Neelam Singh, Manish K. Kansal, Ashwani Kumar, and Vivek Verma, *Mater. Sci. Eng. B*, **282**: 115798 (2022); doi:10.1016/j.mseb.2022.115798
85. Jhilmil Swapnalin, Bhargavi Koneru, P. Banerjee, Srinivasan Natarajan, and A. Franco Jr., *J. Phys. Chem. Solids*, **168**: 110797 (2022); doi:10.1016/j.jpcs.2022.110797
86. Chi Yu, Junhao Peng, Jianhua Guo, Zhenhang Yin, Shixuan Lv, and Xinghua Jiang, *ACS Appl. Electron. Mater.*, **4**: Iss. 11: 5582 (2022); doi:10.1021/acsaelm.2c01168
87. Siyao Guo, Hailong Guan, Ying Li, Yunfeng Bao, Dongyi Lei, Tiejun Zhao, Baomin Zhong, and Zhihong Li, *J. Alloys Compd.*, **887**: 161298 (2021); doi:10.1016/j.jallcom.2021.161298
88. Dawei Liu, Rong Qiang, Yunchen Du, Ying Wang, Chunhua Tian, and Xijiang Han, *J. Colloid Interface Sci.*, **514**: 10 (2018); doi:10.1016/j.jcis.2017.12.013
89. Yan Wang, Xiang Gao, Chenghao Lin, Liyuan Shi, Xuanhua Li, and Guanglei Wu, *J. Alloys Compd.*, **785**: 765 (2019); doi:10.1016/j.jallcom.2019.01.271
90. Nikolaos Kostoglou, Christian Koczwara, Christian Prehal, Velislava Terziyska, Biljana Babic, Branko Matovic, Georgios Constantinides, Christos Tampaxis, Georgia Charalambopoulou, Theodore Steriotis, Steve Hinder, Mark Baker, Kyriaki Polychronopoulou, Charalabos Doumanidis, Oskar Paris, Christian

Mitterer, and Claus Rebholz, *Nano Energy*, **40**: 49 (2017); doi:10.1016/j.nanoen.2017.07.056

91. Lin Long, Erqi Yang, Xiaosi Qi, Ren Xie, Zhong-chen Bai, Shuijie Qin, Chaoyong Deng, and Wei Zhong, *ACS Sustain. Chem. Eng.*, **8**, Iss. 1: 613 (2020); doi:10.1021/acssuschemeng.9b06205
92. Han Hu, Buyuan Guan, Baoyu Xia, and Xiong Wen (David) Lou, *J. Am. Chem. Soc.*, **137**, Iss. 16: 5590 (2015); doi:10.1021/jacs.5b02465
93. Mingyue Kong, Zirui Jia, Bingbing Wang, Jinlei Dou, Xuehua Liu, Yuhao Dong, Binghui Xu, and Guanglei Wu, *Sustain. Mater. Technol.*, **26**: e00219 (2020); doi:10.1016/j.susmat.2020.e00219
94. Fei Wu, Zihao Liu, Jiqi Wang, Tariq Shah, Pei Liu, Qiuyu Zhang, Baoliang Zhang, *Chem. Eng. J.*, **422**: 130591 (2021); doi:10.1016/j.cej.2021.130591
95. Kishore Chand, Xiao Zhang, and Yujin Chen, *Arabian Journal of Chemistry*, **15**: 104143 (2022); doi:10.1016/j.arabjc.2022.104143